Synthesis and Characterization of a Tetrapodal NO_4^{4-} Ligand and Its Transition Metal Complexes

Jordan C. Axelson,[†] Miguel I. Gonzalez,[†] Katie R. Meihaus,[†] Christopher J. Chang,[*,†,‡,§,∥] and Jeffrey R. Long[*,†,#,&]

[†]Departments of Chemistry, [‡]Molecular and Cell Biology, and [#]Chemical and Biomolecular Engineering and the [§]Howard Hughes Medical Institute, University of California, Berkeley, California 94720, United States

[∥]Chemical Sciences Division and [&]Materials Sciences Division, Lawrence Berkeley National Laboratory, Berkeley, California 94720, United States

Ⓢ *Supporting Information*

ABSTRACT: We present the synthesis and characterization of alkali metal salts of the new tetraanionic, tetrapodal ligand 2,2′-(pyridine-2,6-diyl)bis(2-methylmalonate) ($A_4[PY(CO_2)_4]$, A = Li$^+$, Na$^+$, K$^+$, and Cs$^+$), via deprotection of the neutral tetrapodal ligand tetraethyl 2,2′-(pyridine-2,6-diyl)bis(2-methylmalonate) ($PY(CO_2Et)_4$). The $[PY(CO_2)_4]^{4-}$ ligand is composed of an axial pyridine and four equatorial carboxylate groups and must be kept at or below 0 °C to prevent decomposition. Exposing it to a number of divalent first-row transition metals cleanly forms complexes to give the series $K_2[(PY(CO_2)_4)M(H_2O)]$ (M = Mn^{2+}, Fe^{2+}, Co^{2+}, Ni^{2+}, Zn^{2+}). The metal complexes were comprehensively characterized via single-crystal X-ray diffraction, ^{1}H NMR and UV−vis absorption spectroscopy, and cyclic

voltammetry. Crystal structures reveal that $[PY(CO_2)_4]^{4-}$ coordinates in a pentadentate fashion to allow for a nearly ideal octahedral coordination geometry upon binding an exogenous water ligand. Additionally, depending on the nature of the charge-balancing countercation (Li$^+$, Na$^+$, or K$^+$), the $[(PY(CO_2)_4)M(H_2O)]^{2-}$ complexes can assemble in the solid state to form one-dimensional channels filled with water molecules. Aqueous electrochemistry performed on $[(PY(CO_2)_4)M(H_2O)]^{2-}$ suggested accessible trivalent oxidation states for the Fe, Co, and Ni complexes, and the trivalent Co^{3+} species $[(PY(CO_2)_4)Co(OH)]^{2-}$ could be isolated via chemical oxidation. The successful synthesis of the $[PY(CO_2)_4]^{4-}$ ligand and its transition metal complexes illustrates the still-untapped versatility within the tetrapodal ligand family, which may yet hold promise for the isolation of more reactive and higher-valent metal complexes.
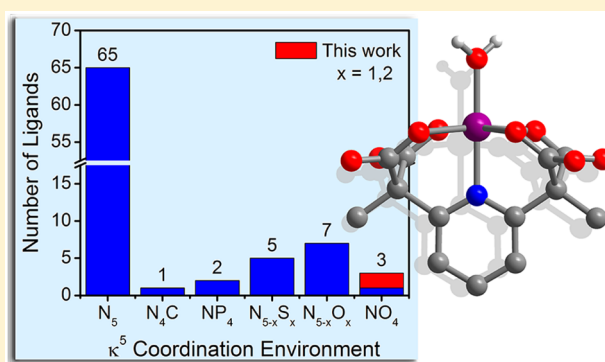
■ INTRODUCTION

Tetrapodal pentadentate ligands are chelators that form square pyramidal coordination caps when bound to a single metal ion.[1] Complexes incorporating these ligands have been studied in a wide variety of applications, for example as hydrogen evolution catalysts,[2] water oxidation catalysts,[3] enzyme mimics,[4,5] redox mediators in dye-sensitized solar cells,[6] and metal cluster systems exhibiting slow magnetic relaxation.[7] In addition to their unique versatility, tetrapodal ligands are advantageous due to their ability to restrict substrate access to a single open coordination site on the metal center and to form discrete, mononuclear complexes with well-defined coordination environments. Moreover, these ligands can afford enhanced stability through the chelate effect compared to their analogous mono- or bidentate counterparts, which is a desirable trait particularly for systems incorporating labile first-row transition metals.[8]

Recently, complexes of the neutral pentadentate ligand 2,6-bis[1,1-bis(2-pyridyl)ethyl]pyridine (PY5Me$_2$) and its derivatives have been extensively investigated in the areas of water reduction catalysis[2] and molecular magnetism.[7a,c] The PY5Me$_2$

ligand exclusively contains pyridine donors, and indeed the vast majority of tetrapodal ligands in the literature contain neutral aliphatic or aromatic nitrogen-donating groups. In contrast, very few tetrapodal scaffolds incorporate carbon-, phosphorus-, oxygen-, or sulfur-based donors, and scaffolds with anionic donors are especially uncommon.[1,9] Given that anionic donors have been shown to facilitate access to high-valent metal complexes,[5,10] a suitable anionic tetrapodal ligand could present an advantageous platform for generating and studying such reactive species. In particular, a primarily anionic oxygen-based environment could engender unique electronic configurations and interesting chemical reactivity due to the different donating capabilities of nitrogen and oxygen.[5,11]

Prior to this work, the only reported tetrapodal ligands exhibiting predominantly oxygen-based environments were the polyalcohols 2,2′-(pyridine-2,6-diyl)bis(2-methylpropane-1,3-diol) (PYO$_4$) and 2-(bis(hydroxymethyl)amino)-2-

(hydroxymethyl)propane-1,3-diol (bis-tris). The crystal structures of PYO$_4$ found in the literature reveal that the ligand is fully protonated and bridges multiple Li$^+$ and Ba^{2+} perchlorate salts instead of binding to the cation in a κ^5 fashion.[12] While bis-tris has been shown to coordinate to transition metals as a pentadentate ligand, it only forms mononuclear complexes as a neutral or 2− ligand[13] and forms clusters when further deprotonated to bear a 3− or 4− charge.[14] We therefore sought to expand this small and unconventional contingent of tetrapodal ligand scaffolds by exploring an all-anionic equatorial oxygen environment.

Herein, we report the synthesis of the tetraanionic ligand 2,2′-(pyridine-2,6-diyl)bis(2-methylmalonate) ([PY(CO$_2$)$_4$]$^{4-}$) via deprotection of the neutral ligand tetraethyl 2,2′-(pyridine-2,6-diyl)bis(2-methylmalonate) (PY(CO$_2$Et)$_4$). The reaction of K$_4$[PY(CO$_2$)$_4$] with divalent first-row transition metals further affords the complexes [(PY(CO$_2$)$_4$)M(H$_2$O)]$^{2-}$ (M = Mn^{2+}, Fe^{2+}, Co^{2+}, Ni^{2+}, Zn^{2+}). Both [PY(CO$_2$)$_4$]$^{4-}$ and PY(CO$_2$Et)$_4$ represent novel additions to the tetrapodal ligand family, and to our knowledge [PY(CO$_2$)$_4$]$^{4-}$ is the first tetraanionic, tetrapodal ligand with an NO$_4$ donor set to successfully form mononuclear complexes with transition metals. We present the synthesis and characterization of the new ligands and comprehensive synthetic, structural, spectroscopic, and electrochemical characterization data for the metal complexes.

■ EXPERIMENTAL SECTION

General Information. Unless specified otherwise, all reactions and manipulations were performed under an inert atmosphere using a glovebox, glovebag, or Schlenk techniques. Dimethylformamide (DMF) and tetrahydrofuran (THF) were dried by passage over activated molecular sieves using a custom-built solvent purification system designed by JC Meyer Solvent Systems. Diethyl malonate, anhydrous 1,4-dioxane (Sigma-Aldrich), and other degassed solvents were purged with N$_2$ for 30−60 min prior to use. All other solvents and reagents were obtained from commercial vendors and utilized without further purification.

Synthesis of Tetraethyl 2,2′-(pyridine-2,6-diyl)bis(2-methylmalonate) (PY(CO$_2$Et)$_4$). An oven-dried Schlenk flask was charged with 2,6-dibromopyridine (14.6 g, 61.5 mmol), CuI (2.34 g, 12.3 mmol), picolinic acid (3.03 g, 24.6 mmol), Cs$_2$CO$_3$ (120 g, 270 mmol), diethyl malonate (40.0 mL, 262 mmol), and 300 mL of anhydrous 1,4-dioxane. The reaction was heated to 80 °C for 14 h. Once cooled, the reaction was quenched with 200 mL of water and extracted four times with 200 mL of ethyl acetate. The organic portions were combined, washed with brine, dried with MgSO$_4$, and concentrated via rotary evaporation to give a yellow oil. The crude product was purified by flash chromatography on silica (3:1 hexanes/ethyl acetate), after which a small amount of side product still remained that could not be removed through additional purification efforts. A ^{1}H NMR spectrum suggested the mixture to be ~5:1 tetraethyl 2,2′-(pyridine-2,6-diyl)dimalonate to impurity (Figure S8). Because this impurity did not substantially impede the synthesis or yield of the desired ligand (see below), the yellow oil obtained from chromatography was dried under reduced pressure and used without further purification in subsequent manipulations. R_f 0.31 (3:1 hexanes/ethyl acetate, UV). ^{1}H NMR (CDCl$_3$, 400 MHz): δ 7.74 (t, J = 7.8 Hz, 1H), 7.48 (d, J = 7.8 Hz, 2H), 4.91 (s, 2H), 4.23 (m, 8H), 1.26 (t, J = 7.1, 12H).

An oven-dried Schlenk flask was charged with the yellow oil containing tetraethyl 2,2′-(pyridine-2,6-diyl)dimalonate (19.1 g), K$_2$CO$_3$ (33.3 g, 241 mmol), methyl iodide (19.5 mL, 313 mmol), and 250 mL of anhydrous DMF, and the mixture was left to stir at room temperature under N$_2$ for 24 h. Subsequently, the flask was cooled to 0 °C in an ice bath, and the reaction was quenched with 200 mL of water followed by 200 mL of Et$_2$O. The organic layer was isolated, and the aqueous layer was extracted three times with 100 mL of Et$_2$O. The organic portions were combined and washed with 150

mL of concentrated Na$_2$SO$_3$ followed by 150 mL of brine. After it was dried with MgSO$_4$, the solution was concentrated to an oily, yellow solid. The crude product was dissolved in a minimal amount of dichloromethane, layered with hexanes, and stored overnight in a −20 °C freezer. Colorless crystals of PY(CO$_2$Et)$_4$ were isolated by vacuum filtration in a 62% yield (16.1 g) with respect to 2,6-dibromopyridine. ^{1}H NMR (CDCl$_3$, 400 MHz): δ 7.63 (t, J = 7.9 Hz, 1H), 7.35 (d, J = 7.9 Hz, 2H), 4.24−4.12 (m, 8H), 1.78 (s, 6H), 1.19 (t, J = 7.1 Hz, 12H). ^{13}C NMR (CDCl$_3$, 400 MHz): δ 170.7, 156.9, 136.5, 121.4, 61.7, 61.6, 22.3, 14.0. IR (neat, cm^{-1}): 2979w, 2937w, 2904w, 2870w, 1758w, 1729s, 1585w, 1576w, 1460m, 1450m, 1387w, 1372m, 1282m, 1244s, 1223s, 1175m, 1161m, 1102s, 1020s, 997m, 953w, 927w, 861m, 823m, 759m, 740w, 713w, 647w, 611m, 515m, 471w. Anal. Calcd for C$_{21}$H$_{29}$NO$_8$: C, 59.56; H, 6.90; N, 3.31%. Found: C, 59.42; H, 6.78; N, 3.55%.

Synthesis of [(PY(CO$_2$Et)$_4$)Cu(THF)](CF$_3$SO$_3$)$_2$. Solid portions of Cu(CF$_3$SO$_3$)$_2$ (71.0 mg, 0.196 mmol) and PY(CO$_2$Et)$_4$ (82.7 mg, 0.195 mmol) were weighed into separate 20 mL vials, and 1.5 mL of THF was added to each vial. Once the PY(CO$_2$Et)$_4$ had dissolved, the two solutions were combined and heated to 60 °C for 2 h to dissolve all reagents. The vial was then left to stir at ambient temperature overnight. Any remaining particulate was removed by vacuum filtration, and the filtrate was concentrated. Blue crystals (96.0 mg, 57% yield) suitable for X-ray analysis were obtained by slow diffusion of ether into the concentrated THF solution at room temperature over 2 d. IR (neat, cm^{-1}): 2984w, 2941w, 2903w, 1692s, 1640m, 1598w, 1460w, 1414w, 1372m, 1325m, 1262s, 1222s, 1182w, 1149s, 1112m, 1091w, 1067w, 1031s, 1010s, 932m, 912m, 864s, 819w, 790w, 753w, 637s, 570s, 516s, 478w, 469w, 461w, 455w. Anal. Calcd for C$_{27}$H$_{37}$CuF$_6$NO$_{15}$S$_2$: C, 37.83; H, 4.35; N, 1.63%. Found: C, 37.61; H, 4.34; N, 1.90%.

Synthesis of 2,2′-(Pyridine-2,6-diyl)bis(2-methylmalonate) salts (A$_4$[PY(CO$_2$)$_4$], A = Li$^+$, Na$^+$, K$^+$, Cs$^+$). In air, PY(CO$_2$Et)$_4$ (120 mg, 0.28 mmol) was dissolved in 13 mL of methanol and cooled to 0 °C. Five equivalents of AOH (A = Li$^+$, Na$^+$, K$^+$, Cs$^+$) in deionized water (1.5 mL of a 0.95 M stock solution) were subsequently added dropwise to the methanol solution. After it was stirred for 6 h, the reaction solution was purged with N$_2$ to evaporate the solvent, all the while ensuring that the temperature remained at or below 0 °C. Although a small amount of side product was observed via ^{1}H NMR spectroscopy (Figure S9), the crude product was used without further purification in the synthesis of the metal complexes. Because of the extra equivalent of unreacted AOH, the isolated white solid was treated as A$_4$[PY(CO$_2$)$_4$]·AOH for stoichiometric purposes in the synthesis of the complexes. ^{1}H NMR (D$_2$O, 400 MHz): δ 7.62 (t, J = 7.9 Hz, 1H), 7.26 (d, J = 7.9 Hz, 2H), 1.72 (s, 6H). ^{13}C NMR (D$_2$O, 400 MHz): δ 181.4, 161.2, 136.7, 120.4, 66.8, 23.2. IR (neat, cm^{-1}): 3349m, 3283m, 2977w, 2945w, 1677w, 1560s, 1451m, 1414m, 1392m, 1326s, 1171w, 1135w, 1100w, 1081w, 994w, 986w, 932w, 901w, 821m, 792w, 762w, 749m, 691m, 641m, 618s, 532s.

General Synthesis of K$_2$[(PY(CO$_2$)$_4$)M(H$_2$O)] Complexes. In air, a 20 mL vial was charged with the crude K$_4$[PY(CO$_2$)$_4$]·KOH (200−400 mg) and 1 equiv of divalent metal chloride (ZnCl$_2$) or divalent metal chloride hydrate (MnCl$_2$·4H$_2$O, FeCl$_2$·4H$_2$O, CoCl$_2$·6H$_2$O, NiCl$_2$·6H$_2$O). The vial was topped with a rubber septum and purged with N$_2$ for 30 min before 5−10 mL of degassed, deionized water was added to the vial via syringe. After the solution had stirred at room temperature for 30 min, the vial was transferred to an N$_2$-filled glovebag, and the solution was vacuum-filtered. Subsequently, 40−80 mL of degassed acetone was added to the filtrate to precipitate the product. The solids were isolated by vacuum filtration, dissolved in a minimal amount of water, and recrystallized by diffusion of acetone into the aqueous solution, which produced block crystals suitable for X-ray analysis. Note that the synthesis and handling of the Ni^{2+} and Zn^{2+} complexes can be performed entirely in air. Lower yields for the Mn^{2+} and Fe^{2+} complexes were attributed to their air sensitivity. Yields given below were calculated based on the initial amount of metal chloride salt employed. Special considerations for each complex are noted in their respective sections.

K₂[(PY(CO₂)₄)Mn(H₂O)]. Pale yellow solids (124 mg) were obtained in 42% yield. IR (neat, cm⁻¹): 3246w, 3017w, 2992w, 2950w, 1670w, 1612s, 1577s, 1568s, 1455m, 1435w, 1413m, 1390s, 1358s, 1299s, 1236m, 1221w, 1182w, 1157w, 1110w, 1078w, 1016w, 987w, 919w, 887s, 846m, 825m, 803w, 768s, 653s, 622s, 608s, 592m, 562m, 455w. μ_{eff}(Evans) = 5.6(2)μ_B. Anal. Calcd for C₁₃H₁₁K₂MnNO₉·H₂O: C, 32.78; H, 2.75; N, 2.94%. Found: C, 32.42; H, 2.54; N, 3.06%.

K₂[(PY(CO₂)₄)Fe(H₂O)]. All synthetic manipulations, including the recrystallization, were performed using Schlenk line techniques. Cannula filtrations were performed instead of vacuum filtrations to obtain 85 mg of the yellow product in 30% yield. IR (neat, cm⁻¹): 3316w, 3016w, 2989w, 2948w, 1670w, 1615s, 1570s, 1456m, 1432m, 1388s, 1357s, 1296s, 1240m, 1227m, 1182w, 1159m, 1111w, 1078w, 1020w, 987w, 919m, 888s, 847m, 826m, 768s, 707m, 653s, 624s, 604s, 596s, 581s, 553s, 532m, 458m. μ_{eff}(Evans) = 4.9(1)μ_B. UV–vis–NIR (H₂O): λ_{max} (ε_M, M⁻¹ cm⁻¹) 427 (170), 958 (4) nm. Anal. Calcd for C₁₃FeH₁₁K₂NO₉·H₂O: C, 32.71; H, 2.75; N, 2.93%. Found: C, 32.51; H, 2.52; N, 2.69%.

K₂[(PY(CO₂)₄)Co(H₂O)]. The pink solids were isolated prior to recrystallization and sonicated with 1–2 mL of methanol. Recrystallization afforded 131 mg of product in 59% yield. IR (neat, cm⁻¹): 3326m, 3016w, 2988w, 2948w, 1673w, 1616s, 1572s, 1458m, 1432m, 1419m, 1390s, 1359s, 1299s, 1244m, 1226m, 1185m, 1162m, 1111w, 1079w, 1026w, 988w, 920w, 887s, 849m, 824w, 769s, 713w, 654s, 629s, 608s, 552s, 466m, 457m. μ_{eff}(Evans) = 4.2(2)μ_B. UV–vis–NIR (H₂O): λ_{max} (ε_M, M⁻¹ cm⁻¹) 465 (10), 495 (sh) (9), 525 (sh) (7), 1049 (8) nm. Anal. Calcd for C₁₃CoH₁₁K₂NO₉·0.5H₂O: C, 33.13; H, 2.57; N, 2.97%. Found: C, 33.03; H, 2.35; N, 2.99%.

Li₂[(PY(CO₂)₄)Ni(H₂O)]. Purple solids (68 mg) were obtained in 23% yield. The low yield for this complex was attributed to poor conversion to the Li₄[(PY(CO₂)₄] ligand based on the qualitative observation that more insoluble side products were removed during the first filtration step compared to the other analogues. IR (neat, cm⁻¹): 3601w, 3228w, 3025w, 3007w, 2960w, 1978w, 1638m, 1628m, 1571s, 1458w, 1429s, 1397s, 1364m, 1316s, 1248m, 1226w, 1187w, 1167w, 1081w, 1030w, 927w, 901m, 859m, 805w, 780m, 680m, 625m, 601s, 486s. UV–vis–NIR (H₂O): λ_{max} (ε_M, M⁻¹ cm⁻¹) 575 (4), 751 (3), 940 (19) nm. Anal. Calcd for C₁₃H₁₁Li₂NNiO₉·2.5 H₂O·0.5 LiCl: C, 33.65; H, 3.48; N, 3.02%. Found: C, 33.41; H, 3.17; N, 3.02%.

Na₂[(PY(CO₂)₄)Ni(H₂O)]. In order to remove residual NaCl, the purple solids were recrystallized a second time by slow evaporation of a concentrated aqueous solution of the complex over 2 d, resulting in 274 mg of purple crystals in 70% yield. IR (ATR, cm⁻¹) 3581w, 3418w, 3289m, 3097m, 3003m, 2961m, 2467w, 1591s, 1572s, 1459s, 1437s, 1383s, 1352s, 1312s, 1272s, 1247m, 1189m, 1167m, 1114w, 1079m, 1032m, 994w, 922m, 893s, 866s, 853s, 829s, 801m, 774s, 738m, 662s, 632s, 596s, 540s, 522s, 467s, 458s. UV–vis–NIR (H₂O): λ_{max} (ε_M, M⁻¹ cm⁻¹) 575 (4), 751 (3), 940 (20) nm. Anal. Calcd for C₁₃H₁₁NNa₂NiO₉·5.5H₂O: C, 29.52; H, 4.19; 2.65%. Found: C, 29.69; H, 4.05; N, 2.56%.

K₂[(PY(CO₂)₄)Ni(H₂O)]. Purple solids were isolated prior to recrystallization and sonicated with 1–2 mL of methanol. Recrystallization afforded 170 mg of product in 63% yield. IR (neat, cm⁻¹): 3568w, 3099w, 2982w, 2948w, 2887w, 1618s, 1610s, 1589s, 1577s, 1571s, 1560s, 1535m, 1459m, 1425m, 1383s, 1362s, 1294s, 1281s, 1246s, 1187m, 1166m, 1118w, 1080m, 1030w, 987w, 923m, 892s, 847m, 834m, 809m, 770s, 739m, 716m, 669s, 633s, 601s, 530m, 517m, 470s. μ_{eff}(Evans) = 3.0(1)μ_B. UV–vis–NIR (H₂O): λ_{max} (ε_M, M⁻¹ cm⁻¹) 577 (5), 751 (4), 940 (21) nm. Anal. Calcd for C₁₃H₁₁K₂NNiO₉·H₂O: C, 32.52; H, 2.73; N, 2.92%. Found: C, 32.82; H, 2.46; N, 2.88%.

Cs₂[(PY(CO₂)₄)Ni(H₂O)]. The blue solids were isolated prior to recrystallization and sonicated with 1–2 mL of methanol. Recrystallization afforded 191 mg of product in 60% yield. IR (neat, cm⁻¹): 3142w, 3000w, 2991w, 2942w, 1619s, 1586s, 1575s, 1457m, 1446m, 1421m, 1348s, 1360s, 1290s, 1277s, 1246s, 1187m, 1165m, 1121w, 1079m, 1031w, 988w, 924m, 890s, 847m, 830m, 808w, 766s, 723m, 706m, 689m, 665s, 633s, 600s, 548w, 521w, 476w, 467w, 457w. UV–vis–NIR (H₂O): λ_{max} (ε_M, M⁻¹ cm⁻¹): 575 (4), 751 (4), 939 (21) nm.

Anal. Calcd for C₁₃H₁₁Cs₂NNiO₉: C, 24.03; H, 1.71; N, 2.16%. Found: C, 23.94; H, 1.39; N, 2.04%.

K₂[(PY(CO₂)₄)Zn(H₂O)]. White solids were isolated prior to recrystallization and sonicated with 1–2 mL of methanol. Recrystallization afforded 43 mg of product in 32% yield. ¹H NMR (D₂O, 600 MHz): δ 7.91 (t, J = 8.1 Hz, 1H), 7.57 (d, J = 8.1 Hz, 2H), 1.82 (s, 6H). IR (neat, cm⁻¹): 3012w, 2983w, 2947w, 1636s, 1624s, 1617s, 1610s, 1577s, 1571s, 1560s, 1458m, 1430m, 1382s, 1355m, 1289s, 1258s, 1242s, 1185m, 1164m, 1117w, 1077m, 1023w, 988w, 921m, 892s, 844m, 830m, 803m, 768s, 738m, 674m, 664m, 627s, 599s, 591s, 526m, 510m, 481m, 465m. Anal. Calcd for C₁₃H₁₁K₂NO₉Zn·1.5H₂O: C, 31.49; H, 2.85; N, 2.82%. Found: C, 31.34; H, 2.57; N, 2.73%.

Synthesis of K₂[(PY(CO₂)₄)Co(OH)]. In air, K₂[(PY(CO₂)₄)Co-(H₂O)] (54.0 mg, 0.115 mmol) was dissolved in 4.5 mL of deionized water and filtered to remove any remaining particulate. While the solution was stirred at ambient temperature in a 20 mL vial, 0.3 mL of hydrogen peroxide (34–37% by mass) was slowly added dropwise over 1.5 min. The vial was left to stir uncapped for 24 h, and the solution was then concentrated to 3 mL. Dark purple needles suitable for X-ray analysis were obtained by slow diffusion of acetone into the aqueous solution at room temperature over 3 d. The final product (46.9 mg, 85% yield) was collected by vacuum filtration, and the solids were washed three times with 1.5 mL of methanol. ¹H NMR (D₂O, 400 MHz) δ 8.30 (t, J = 8.1 Hz, 1H), 7.78 (d, J = 8.1 Hz, 2H), 1.83 (s, 6H). IR (neat, cm⁻¹): 3587w, 3094w, 2999w, 2952w, 1705w, 1666s, 1637s, 1589s, 1571s, 1465m, 1428w, 1386s, 1338m, 1312m, 1255m, 1198m, 1171m, 1115w, 1079w, 1044w, 992w, 923m, 897s, 804w, 783s, 741m, 717w, 705w, 675m, 655s, 608s, 568w, 549w, 540w, 521w, 503w, 486s, 455m. UV–vis–NIR (H₂O): λ_{max} (ε_M, M⁻¹ cm⁻¹) 374 (130), 541 (170) nm. Anal. Calcd for C₁₃H₁₀CoK₂NO₉·H₂O: C, 32.57; H, 2.52; N, 2.92%. Found: C, 32.50; H, 2.50; N, 2.89%.

Physical Measurements. ¹H and ¹³C NMR spectra were collected at room temperature (22–25 °C) on Bruker AV-600 MHz, AVB-400 MHz, or AVQ-400 MHz instruments and analyzed with MestReNova software (v8.0.2−11021, Mestrelab Research S.L). All resonances were referenced to the residual solvent signals of CDCl₃ (¹H, 7.26 ppm; ¹³C, 77.16 ppm) or D₂O (¹H, 4.80 ppm). The ¹³C NMR spectrum of [PY(CO₂)₄]⁴⁻ was referenced to CDCl₃ by dissolving [PY(CO₂)₄]⁴⁻ in D₂O and inserting a 2 mm coaxial tube filled with CDCl₃ into the NMR tube. Evans method magnetic measurements[15] were performed using a solvent-standard mixture of 2% acetone in D₂O (v/v) at room temperature (22–25 °C). The μ_{eff} values were calculated by the simplified form recommended by Grant,[16] which excludes solvent correction, and are reported as the average of three samples measured. Diamagnetic contributions were accounted for using Pascal's constants.[17] A Cary 5000 UV−vis−NIR spectrophotometer and Cary WinUV v3.0 software were used to obtain spectra of solution samples in water and diffuse reflectance spectra of solid samples mixed with poly(vinylidene fluoride). A Kubelka−Munk conversion was applied to the diffuse reflectance spectra. Infrared spectra were collected on a PerkinElmer Spectrum 400 FT-IR spectrometer using the attenuated total reflectance mode. C, H, and N elemental analyses were performed in the Microanalytical Laboratory of the University of California, Berkeley.

Electrochemical Measurements. Electrochemical measurements were made with a BioLogic SP-200 potentiostat using the EC-Lab v10.37 software. Experiments were performed under an argon atmosphere in a single compartment cell using a glassy carbon working electrode, Ag/AgCl (3.0 M NaCl) reference electrode, and platinum wire counter electrode. An aqueous solution of 0.1 M KClO₄ was used as the electrolyte. The pH of the electrolyte solutions was adjusted using KOH and HCl. Between each scan, the working electrode was removed from solution and polished with 0.05 μm MicroPolish (CH Instruments, Inc).

Crystallography. Crystallography was performed at the Small Molecule X-ray Crystallography Facility at the University of California, Berkeley, and the Advanced Light Source at Lawrence Berkeley National Laboratory. X-ray data were collected on single crystals coated with paratone oil and mounted on Kapton or MiTeGen loops. All data collections were performed at 100 K using a Bruker QUAZAR

Scheme 1. Synthesis of Divalent Transition Metal Complexes $[(PY(CO_2)_4)M(H_2O)]^{2-}$ ($M = Mn^{2+}$, Fe^{2+}, Co^{2+}, Ni^{2+}, Zn^{2+})
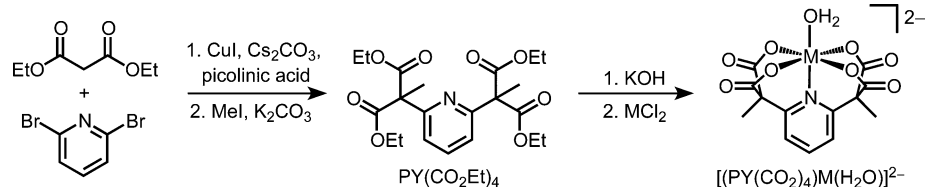
diffractometer equipped with a microfocus sealed X-ray source of Mo Kα (λ = 0.710 73 Å) radiation and a Bruker APEX-II detector; a Bruker APEX diffractometer equipped with a fine-focus sealed X-ray source of Mo Kα (λ = 0.710 73 Å) radiation and a Bruker APEX-I detector; or at Beamline 11.3.1 at the Advanced Light Source using synchrotron radiation with either a Bruker AXS APEX II CCD detector or a Bruker PHOTON100 CMOS detector on a Bruker D8 Diffractometer. Raw data were integrated and corrected for Lorentz and polarization effects using Bruker APEX2 V. 2011.4 software.[18] Absorption corrections were applied using SADABS[19] or TWINABS.[20] Space group assignments were determined by examination of systematic absences, E-statistics, and successive refinement of the structures. All structures were solved by direct methods using SHELXT.[21] Additional refinement was performed with SHELXL-2014/7[22] operated through the WinGX[23] and OLEX2[24] interfaces. Molecular graphics were generated with DIAMOND.[25] None of the crystals showed significant decay during data collection. Specific details concerning each data set can be found in the Supporting Information.

■ RESULTS AND DISCUSSION

In our design of a tetraanionic pentadentate scaffold, we targeted functional groups resistant to oxidative decomposition such as carboxylates and phenolates, as both could withstand the conditions required for the formation of high-valent metal complexes. Ultimately, we chose to focus on a carboxylate-based ligand, as it could be readily designed to retain a binding pocket analogous to that of $PY5Me_2$. However, while the addition of the peripheral pyridine rings during the synthesis of $PY5Me_2$ is well-established and proceeds though a simple S_NAr reaction,[7c,26] the installation of equatorial carboxylate moieties is less straightforward.

Retrosynthetically, the most direct way to achieve oxygen donors at positions matching those of the pyridine nitrogen atoms in $PY5Me_2$ is to connect two malonate functional groups to the central pyridine. A review of potential routes revealed three methods most amenable to this aim: (i) activation of pyridine-N-oxide with the phosphonium salt PyBroP,[27] (ii) synthesis of a linear 1,5-dicarbonyl precursor with subsequent oxidation to a pyridine ring,[28] or (iii) a copper-catalyzed Ullman-type reaction with 2,6-dibromopyridine.[29] Although we were able to add a single malonate unit to pyridine-N-oxide with PyBroP, a second addition was not observed upon further reaction of the monosubstituted pyridine-N-oxide intermediate under the same conditions. Additionally, while we were able to isolate the linear precursor tetraethyl 2,6-dioxoheptane-1,1,7,7-tetracarboxylate, exposure of this molecule to the amine sources needed to close the ring (NH_3, NH_4OH, NH_4OAc, or NH_2OH) only resulted in decarboxylation of the diethyl malonate components, even at room temperature. Ultimately, we found the Ullman-type reaction to be the most successful, and requiring shorter reaction times than originally reported.[29]

Utilizing this latter strategy, the tetraester ligand $PY(CO_2Et)_4$ was generated via a two-step synthesis from 2,6-dibromopyridine (Scheme 1). In the first step, a copper-catalyzed Ullman-type reaction substituted both bromine atoms on the pyridine

with diethyl malonate units. Attempts were also made with diethyl methylmalonate; however, no reaction was observed. The majority of unwanted side products were then removed from the crude oil via column chromatography. One impurity that could not be completely eliminated, however, was likely the asymmetric decomposition product formed by the loss of a single ester group (see the ^1H NMR spectrum of the chromatographed oil, Figure S8). In spite of this impurity, methylation at the tertiary carbon was performed successfully with methyl iodide and K_2CO_3 at room temperature under N_2 in anhydrous DMF. Pure $PY(CO_2Et)_4$ was isolated as a white solid in 62% yield (based on 2,6-dibromopyridine) after recrystallization from a dichloromethane solution layered with hexanes and stored at −20 °C overnight. The ester ligand is soluble in ethereal, halogenated, and polar organic solvents such as acetone and methanol, and it can be stored indefinitely at room temperature.

Although not our final tetraanionic ligand target, we were interested in the possibility of isolating metal complexes based on the weakly donating environment of $PY(CO_2Et)_4$. While air-free reactions of $PY(CO_2Et)_4$ with halide and triflate salts of Mn^{2+}, Fe^{2+}, Fe^{3+}, and Co^{2+} showed no reaction, the combination of $PY(CO_2Et)_4$ with 1 equiv of $Cu(CF_3SO_3)_2$ under N_2 in anhydrous THF resulted in the formation of a blue solution. Diffusion of diethyl either into this solution at room temperature yielded pale blue crystals of $[(PY(CO_2Et)_4)Cu(THF)](CF_3SO_3)_2$. More coordinating solvents such as acetonitrile could not be used in recrystallization, as they displaced the tetrapodal ligand from the metal center. A crystal structure determination confirmed that the ligand binds in a κ^5 fashion through the axial pyridine and the four carbonyls of the ester groups (Figure 1). A molecule of THF fills the open coordination site to yield a distorted octahedral coordination geometry, while two outer-sphere trifluoromethanesulfonate counteranions confirm the presence of divalent copper. Unlike most octahedral Cu^{2+} complexes, the distortion akin to a Jahn–Teller effect manifests as a compression along the z-axis of the molecule: the average bond length of the equatorial esters is
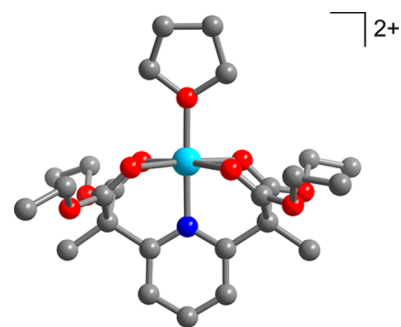

Figure 1. X-ray crystal structure of $[(PY(CO_2Et)_4)Cu(THF)]^{2+}$. Cyan, red, blue, and gray spheres represent Cu, O, N, and C, respectively; H atoms and counterions were omitted for clarity.

Table 1. Crystallographic Data for $K_2[(PY(CO_2)_4)M(H_2O)]$ Complexes with Selected Bond Lengths (Å) and Angles (deg)

M	Mn^{2+}	Fe^{2+}	Co^{2+}	Ni^{2+}	Zn^{2+}
formula	$C_{13}H_{13}K_2MnNO_{10}$	$C_{13}H_{15}FeK_2NO_{11}$[a]	$C_{13}H_{13}CoK_2NO_{10}$	$C_{13}H_{15}K_2NNiO_{11}$[a]	$C_{13}H_{15}K_2NO_{11}Zn$[a]
crystal system	orthorhombic	triclinic	orthorhombic	triclinic	triclinic
space group	$Pnna$	$P\bar{1}$	$Pnna$	$P\bar{1}$	$P\bar{1}$
$M-O_{eq}$, Å[b]	2.1405(16)	2.0945(1)	2.0678(17)	2.0321(18)	2.0790(3)
$M-O_{water}$, Å	2.125(3)	2.1041(1)	2.070(3)	2.0645(18)	2.063(2)
$M-N_{PY}$, Å	2.210(3)	2.1247(1)	2.067(3)	2.011(2)	2.092(3)
$O_{ax}-M-N_{PY}$, deg	180	178.37(17)	180	178.89(8)	178.83(4)
PY-tilt, deg[c]	90	89.730(157)	90	88.195(68)	89.147(107)
OOP distortion, Å[d]	0.2924(12)	0.1377(16)	0.1330(12)	0.0515(9)	0.1195(11)

[a]Protons belonging to all water molecules are included in the chemical formula here, though they were omitted from the refinement of the data set. [b]Average of the four equatorial M−O distances. [c]The PY-tilt is defined as the angle between the least-squares planes generated by the four equatorial oxygen donors and the atoms of the pyridine ring. [d]The out-of-plane (OOP) distortion is defined as the displacement of the metal center from the least-squares plane generated by the four equatorial oxygen atoms.
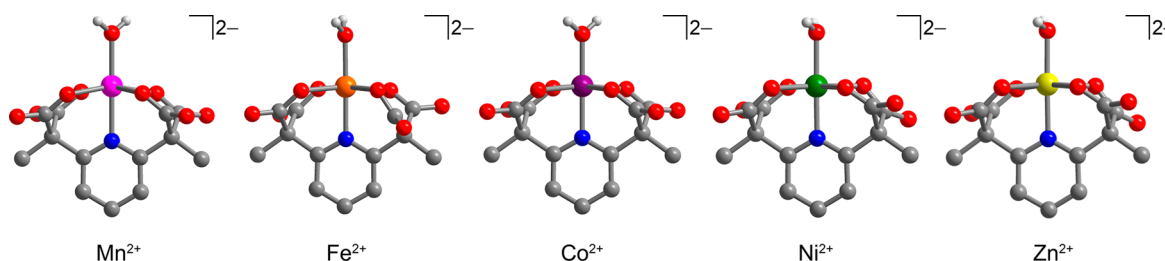

Figure 2. X-ray crystal structures of $[(PY(CO_2)_4)M(H_2O)]^{2-}$ complexes. Magenta, orange, purple, green, yellow, red, blue, gray, and light gray spheres represent Mn, Fe, Co, Ni, Zn, O, N, C, and H atoms, respectively. Water H atoms were identified from the electron density map. All other H atoms and counterions were omitted for clarity.

2.114(2) Å, while the Cu−O$_{THF}$ and Cu−N$_{PY}$ bond lengths are 1.943(2) and 1.990(2) Å, respectively. This axial compression and resultant destabilization of the d_{z^2}, d_{xz}, and d_{yz} orbitals is attributed to the stronger donor properties of the pyridyl nitrogen as compared to the weaker carbonyl oxygens of the esters.

Salts of the tetracarboxylate ligand $A_4[PY(CO_2)_4]$ (A = Li⁺, Na⁺, K⁺, Cs⁺) were synthesized via deprotection of the $PY(CO_2Et)_4$ ester groups with hydroxide in a mixture of 9:1 methanol to water at 0 °C. Compounds of the type $A_4[PY(CO_2)_4]$ could be obtained from reactions with LiOH, NaOH, KOH, or CsOH, while conversion attempts with $(NBu_4)OH$ were unsuccessful. A ¹H NMR spectrum of the product obtained via conversion with $(NBu_4)OH$ revealed the loss of two carboxylate moieties, thus suggesting that the alkali metal hydroxides are necessary for preservation of the ligand. The alkali metal salts of $[PY(CO_2)_4]^{4-}$ appear to be quite temperature sensitive, and significant decomposition could be observed in the ¹H NMR spectrum when the reaction was performed even at room temperature. This sensitivity is likely due to the propensity of malonate functional groups toward decarboxylation. However, it was found that $A_4[PY(CO_2)_4]$ salts could be reproducibly synthesized by maintaining a temperature at or below 0 °C throughout the reaction and during subsequent solvent removal. The purification of $A_4[PY(CO_2)_4]$ salts also proved challenging due to this temperature sensitivity. Consequently the as-synthesized material was combined immediately with 1 equiv of divalent metal chloride in water to obtain the complex salts $K_2[(PY(CO_2)_4)M(H_2O)]$ (M = Mn^{2+}, Fe^{2+}, Co^{2+}, Ni^{2+}, Zn^{2+}).[30] Any impurities carried over from the ligand synthesis were subsequently removed by filtration and recrystallization to give the pure metal complex. In the case of Ni^{2+} and Zn^{2+}, the metalation

could be performed at room temperature in air, and the resulting compounds are quite robust and can be stored indefinitely in air at room temperature. For Mn^{2+}, Fe^{2+}, and Co^{2+}, it was necessary to perform all reactions and subsequent manipulations under an inert atmosphere. The potassium salts of these complexes are soluble in water and completely insoluble in the organic solvents methanol, acetonitrile, and acetone. Aqueous UV−vis−NIR spectra for all the complexes exhibit low-ε intensity absorption bands consistent with Laporte-forbidden d−d transitions (Figure S11).

Diffusion of acetone into concentrated aqueous solutions of all the complexes resulted in block-shaped X-ray quality crystals, and the metrical data from diffraction studies are given in Table 1.[31] All of the complexes are isostructural and exhibit a distorted octahedral geometry arising from penta-dentate coordination of $[PY(CO_2)_4]^{4-}$ and an axially bound water molecule (Figure 2). For the paramagnetic ions, all metal−ligand bond distances are within the expected ranges for octahedral, high-spin complexes,[5,32] while magnetic moments determined using the Evans method[15−17] further support the high-spin assignments.[33] The metal−ligand distances decrease across the series from Mn^{2+} to Ni^{2+}, in accordance with the expected trend based on ionic radii, as does the extent to which the metal cation distorts out of the equatorial ligand plane. For example, the Mn^{2+} cation projects nearly 0.3 Å out of the binding pocket while the same distortion for Ni^{2+} is only 0.05 Å, suggesting that smaller transition metal ions are better accommodated by $[PY(CO_2)_4]^{4-}$.

Crystal structure determinations also revealed some intriguing extended structures for these carboxylate-rich complexes. Indeed, pyridyl π−π stacking and potassium bridging between adjacent complexes generates a three-dimensional network with channels extending along the crystallographic a-axis that are
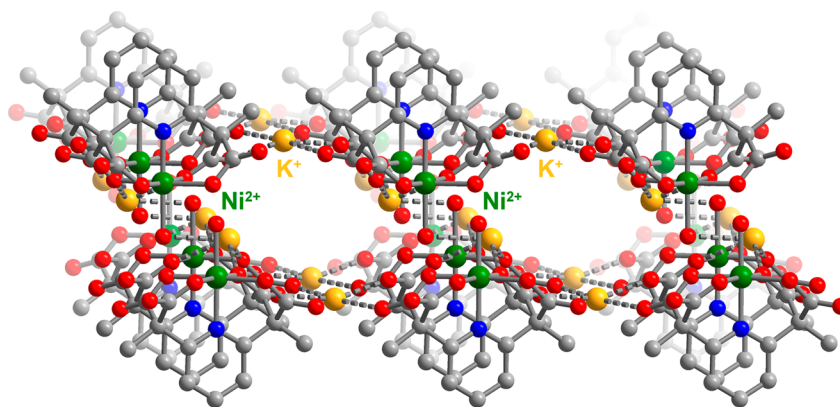
Figure 3. Extended structure of $K_2[(PY(CO_2)_4)Ni(H_2O)]$ viewed along the *a*-axis. Green, light yellow, red, blue, and gray spheres represent Ni, K, O, N, and C atoms, respectively. Water molecules coordinated to K^+ were removed to accentuate the channels. All H atoms were omitted for clarity.

filled with water molecules bound to the bridging cations (see Figure 3). Synthesis and solid-state characterization of the series $A_2[(PY(CO_2)_4)Ni(H_2O)]$ ($A = Li^+$, Na^+, and Cs^+), in the manner described above for $A = K^+$, revealed that the identity of the countercation has a substantial influence on the molecular packing.[34] Indeed, although the immediate coordination environment of the Ni^{2+} centers varies only slightly (Table S9), the mode of alkali metal ion coordination influences the resultant channel formation, size, and solvent occupancy. For example, the height of the channels in the K^+ compound ($K^+ \cdots K^+$) is 6.935(3) Å ($Ni^{2+} \cdots Ni^{2+}$ = 10.3400(5) Å)[35] with two water molecules per formula unit. In comparison, though it contains more water molecules (2.5 per formula unit, Figure S25), the channel height in the Li^+ structure ($Li^+ \cdots Li^+$) is only 4.5691(9) Å ($Ni^{2+} \cdots Ni^{2+}$ = 7.356(2) Å). The channel of the Na^+ analogue is the largest in size, with a $Na^+ \cdots Na^+$ separation of 11.044(2) Å ($Ni^{2+} \cdots Ni^{2+}$ = 13.371(3) Å). Six extra solvent molecules occupy each formula unit in this expanded volume, and one Na^+ ion is completely solvated by water (Figure S26). In contrast to the other three structures, $Cs_2[(PY(CO_2)_4)Ni(H_2O)]$ does not exhibit channels, and packing does not accommodate water outside of the Ni^{2+} coordination sphere (Figure S28).

Encouraged by the successful metalation of $[(PY(CO_2)_4)]^{4-}$, we further sought to enhance the solubility of the $[(PY(CO_2)_4)M(H_2O)]^{2-}$ complexes in organic solvents by exchanging K^+ with aliphatic cations. Indeed, if this ligand scaffold were capable of supporting a high-valent metal center, the ability to utilize a more inert solvent system with a wider electrochemical window would aid in the isolation and reactivity studies of such a species. Because of their ease of handling in air, we first performed salt metathesis with $K_2[(PY(CO_2)_4)Ni(H_2O)]$ and $K_2[(PY(CO_2)_4)Zn(H_2O)]$ via reaction with one equivalent of bis-(triphenylphosphoranylidene)ammonium (PPN^+) chloride in a 3:1 mixture of water/ethanol. The transparent mixtures were then left to stand open to air, and over the course of 2−3 d the ethanol evaporated to yield colorless (Zn^{2+}) and pale purple (Ni^{2+}) needles. Elemental analysis of both the Ni^{2+} and Zn^{2+} products and single-crystal X-ray characterization of the Zn^{2+} complex (Figure S24) confirmed successful cation exchange. The resulting PPN^+ salts are indeed soluble in a number of organic solvents (e.g., methanol, acetonitrile, acetone, and dichloromethane); however, the complexes decompose rapidly in solution at room temperature, precluding further study under these conditions (see Supporting Information for details).

Consequently, aqueous cyclic voltammetry was performed on the series of $[PY(CO_2)_4]^{4-}$ metal complexes at pH 7 in 0.1 M $KClO_4$ electrolyte solution to examine the impact of the tetraanionic donor on the redox potentials. The Zn^{2+} complex exhibited no redox activity from −1.5 to 1.5 V versus Ag/AgCl, confirming that $[PY(CO_2)_4]^{4-}$ is not electrochemically active within this range. As shown in Figure 4, quasireversible 3+/2+
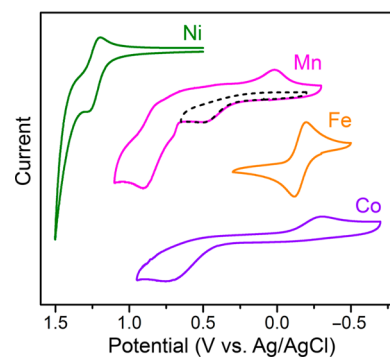

Figure 4. Cyclic voltammograms of $K_2[(PY(CO_2)_4)M(H_2O)]$ complexes in pH 7 aqueous solution with 0.1 M $KClO_4$ electrolyte. All scans were performed at 100 mV sec^{-1}. $M = Mn^{2+}$ (magenta), Fe^{2+} (orange), Co^{2+} (purple), and Ni^{2+} (green).

redox couples were observed for the Fe^{2+} and Ni^{2+} complexes with $E_{1/2}$ values of −0.16 and 1.24 V, respectively, though neither of these redox events exhibited pH dependence from pH = 7−10. In the case of the Co^{2+} complex, an irreversible oxidation occurred at 0.74 V and was followed by an irreversible reduction at −0.30 V on the return scan. This cathodic feature was only observed after initial oxidation of $[(PY(CO_2)_4)Co(H_2O)]^{2-}$. In an effort to identify the oxidized species, we also performed cyclic voltammetry on the low-spin complex $[(PY(CO_2)_4)Co(OH)]^{2-}$, which is formed cleanly via chemical oxidation of $[(PY(CO_2)_4)Co(H_2O)]^{2-}$ with H_2O_2.[36] This experiment revealed a cathodic trace identical to that of $[(PY(CO_2)_4)Co(H_2O)]^{2-}$, which suggests that the oxidation of $[(PY(CO_2)_4)Co(H_2O)]^{2-}$ at 0.74 V is accompanied by deprotonation of the aquo ligand. The separation of the anodic and cathodic peak potentials by more than 1 V is likely due to stabilization of Co^{3+} by the resultant hydroxide moiety as well as to the low- to high-spin conversion mediated by the reduction.

Cyclic voltammograms of the Mn^{2+} complex were more complex than the other compounds. An initial irreversible anodic feature was present with $E_{pa} = 0.50$ V and was assigned as the oxidation of the Mn^{2+} complex to a Mn^{3+} species. Upon scanning to higher potentials, another anodic feature appeared at 0.90 V with a peak current more than twice that of the oxidation occurring at 0.50 V. A subtle shoulder in this second feature suggested at least two overlapping oxidations in this region. These oxidations were not electrochemically reversible, and higher-valent manganese species could not be isolated via chemical oxidation; thus, it was not possible to definitively identify the oxidized products. After the oxidation at 0.90 V, a further reduction at 0.02 V, not associated with the initial feature at 0.50 V, appeared on the return cathodic scan.

CONCLUSIONS

Two new tetrapodal ligands, $PY(CO_2Et)_4$ and $[PY(CO_2)_4]^{4-}$, were synthesized and metalated with first-row transition metals to generate the octahedral complexes $[(PY(CO_2Et)_4)Cu-(THF)]^{2+}$ and $[(PY(CO_2)_4)M(H_2O)]^{2-}$ (M = Mn^{2+}, Fe^{2+}, Co^{2+}, Ni^{2+}, Zn^{2+}). In particular, $[PY(CO_2)_4]^{4-}$ provides the first example of a tetraanionic, tetrapodal framework capable of forming mononuclear complexes, and although it is moderately temperature sensitive as an alkali metal salt, its stability is significantly enhanced when bound to divalent transition metal cations. X-ray structural characterization of the complex salts $K_2[(PY(CO_2)_4)M(H_2O)]$ verified that the ligand chelates in a κ^5 fashion and that the binding pocket is best suited for smaller divalent cations such as Ni^{2+}. The packing of the transition metal complexes in the solid state further revealed a unique three-dimensional network that is dependent on the nature of the charge balancing alkali metal cation. Aqueous cyclic voltammetry experiments further established accessible trivalent oxidation states for the Fe, Co, and Ni complexes. Though, in our hands only the Co^{3+} species $[(PY(CO_2)_4)Co(OH)]^{2-}$ was isolated and structurally characterized. While it was not possible to solubilize $[(PY(CO_2)_4)M(H_2O)]^{2-}$ in organic solvents and probe even higher oxidation states, this work importantly highlights the tunability of the tetrapodal ligand framework and suggests that even more exotic ligand variations capable of generating new reactive metal complexes are within reach.

ASSOCIATED CONTENT

⑤ Supporting Information

The Supporting Information is available free of charge on the ACS Publications website at DOI: 10.1021/acs.inorgchem.6b00908.

> Figures as labeled in the text, additional experimental procedures, single-crystal X-ray diffraction data, and UV−vis−NIR absorption spectral data. (PDF)
> Crystallographic data in CIF format. (ZIP)

AUTHOR INFORMATION

Corresponding Authors
*E-mail: chrischang@berkeley.edu. (C.J.C.)
*E-mail: jrlong@berkeley.edu. (J.R.L.)
Notes
The authors declare no competing financial interest.

ACKNOWLEDGMENTS

REFERENCES

(1) Grohmann, A. *J. Chem. Soc., Dalton Trans.* **2010**, *39*, 1432−1440.
(2) (a) Karunadasa, H. I.; Chang, C. J.; Long, J. R. *Nature* **2010**, *464*, 1329−1333. (b) Sun, Y.; Bigi, J. P.; Piro, N. A.; Tang, M. L.; Long, J. R.; Chang, C. J. *J. Am. Chem. Soc.* **2011**, *133*, 9212−9215. (c) Karunadasa, H. I.; Montalvo, E.; Sun, Y.; Majda, M.; Long, J. R.; Chang, C. J. *Science* **2012**, *335*, 698−702. (d) Thoi, V. S.; Karunadasa, H. I.; Surendranath, Y.; Long, J. R.; Chang, C. J. *Energy Environ. Sci.* **2012**, *5*, 7762−7770. (e) Sun, Y.; Sun, J.; Long, J. R.; Yang, P.; Chang, C. J. *Chem. Sci.* **2013**, *4*, 118−124. (f) Thoi, V. S.; Sun, Y.; Long, J. R.; Chang, C. J. *Chem. Soc. Rev.* **2013**, *42*, 2388−2400. (g) King, A. E.; Surendranath, Y.; Piro, N. A.; Bigi, J. P.; Long, J. R.; Chang, C. J. *Chem. Sci.* **2013**, *4*, 1578−1587. (h) Zee, D. Z.; Chantarojsiri, T.; Long, J. R.; Chang, C. J. *Acc. Chem. Res.* **2015**, *48*, 2027−2036.
(3) (a) Wasylenko, D. J.; Ganesamoorthy, C.; Borau-Garcia, J.; Berlinguette, C. P. *Chem. Commun.* **2011**, *47*, 4249−4251. (b) Wasylenko, D. J.; Palmer, R. D.; Schott, E.; Berlinguette, C. P. *Chem. Commun.* **2012**, *48*, 2107−2109. (c) Wang, L.; Duan, L.; Ambre, R. B.; Daniel, Q.; Chen, H.; Sun, J.; Das, B.; Thapper, A.; Uhlig, J.; Dinér, P.; Sun, S. *J. Catal.* **2016**, *335*, 72−78.
(4) (a) Goldsmith, C. R.; Jonas, R. T.; Stack, T. D. P. *J. Am. Chem. Soc.* **2002**, *124*, 83−96. (b) Que, L. *Acc. Chem. Res.* **2007**, *40*, 493−500. (c) McQuilken, A. C.; Ha, Y.; Sutherlin, K. D.; Siegler, M. A.; Hodgson, K. O.; Hedman, B.; Solomon, E. I.; Jameson, G. N. L.; Goldberg, D. P. *J. Am. Chem. Soc.* **2013**, *135*, 14024−14027.
(5) McDonald, A. R.; Guo, Y.; Vu, V. V.; Bominaar, E. L.; Münck, E.; Que, L. *Chem. Sci.* **2012**, *3*, 1680−1693.
(6) Kashif, M. K.; Axelson, J. C.; Duffy, N. W.; Forsyth, C. M.; Chang, C. J.; Long, J. R.; Spiccia, L.; Bach, U. *J. Am. Chem. Soc.* **2012**, *134*, 16646−16653.
(7) (a) Freedman, D. E.; Jenkins, D. M.; Iavarone, A. T.; Long, J. R. *J. Am. Chem. Soc.* **2008**, *130*, 2884−2885. (b) Atanasov, M.; Busche, C.; Comba, P.; El Hallak, F.; Martin, B.; Rajaraman, G.; van Slageren, J.; Wadepohl, H. *Inorg. Chem.* **2008**, *47*, 8112−8125. (c) Bechlars, B.; D'Alessandro, D. M.; Jenkins, D. M.; Iavarone, A. T.; Glover, S. D.; Kubiak, C. P.; Long, J. R. *Nat. Chem.* **2010**, *2*, 362−368.
(8) Grohmann, A. Tetrapodal Pentadentate Nitrogen Ligands: Aspects of Complex Structure and Reactivity. In *Advances in Inorganic Chemistry*; van Eldik, R., Olabe, J. A., Eds.; Academic Press: 2004; Vol. 56, pp 179−210.
(9) See Figures S1 and S2 for a distribution of coordination environments and net formal charges of donor atoms found in tetrapodal ligands that have been deposited in the Cambridge Crystallographic database.
(10) (a) Lomoth, R.; Huang, P.; Zheng, J.; Sun, L.; Hammarström, L.; Åkermark, B.; Styring, S. *Eur. J. Inorg. Chem.* **2002**, *2002*, 2965−2974. (b) Xu, Y.; Åkermark, T.; Gyollai, V.; Zou, D.; Eriksson, L.; Duan, L.; Zhang, R.; Åkermark, B.; Sun, L. *Inorg. Chem.* **2009**, *48*, 2717−2719. (c) Duan, L.; Fischer, A.; Xu, Y.; Sun, L. *J. Am. Chem. Soc.* **2009**, *131*, 10397−10399. (d) Chantarojsiri, T.; Sun, Y.; Long, J. R.; Chang, C. J. *Inorg. Chem.* **2015**, *54*, 5879−5887.
(11) (a) Pestovsky, O.; Stoian, S.; Bominaar, E. L.; Shan, X.; Münck, E.; Que, L.; Bakac, A. *Angew. Chem.* **2005**, *117*, 7031−7034. (b) Xiao,

D. J.; Bloch, E. D.; Mason, J. A.; Queen, W. L.; Hudson, M. R.; Planas, N.; Borycz, J.; Dzubak, A. L.; Verma, P.; Lee, K.; Bonino, F.; Crocellà, V.; Yano, J.; Bordiga, S.; Truhlar, D. G.; Gagliardi, L.; Brown, C. M.; Long, J. R. *Nat. Chem.* **2014**, *6*, 590−595.

(12) (a) Schmidt, S.; Omnes, L.; Heinemann, F. W.; Kuhnigk, J.; Krüger, C.; Grohmann, A. *Z. Naturforsch., B: J. Chem. Sci.* **1998**, *53*, 946−954. (b) Zimmermann, C.; Bauer, W.; Heinemann, F. W.; Grohmann, A. *Z. Naturforsch., B: Chem. Sci.* **2002**, *57*, 1256−1264.

(13) (a) Inomata, Y.; Gochou, Y.; Nogami, M.; Howell, F. S.; Takeuchi, T. *J. Mol. Struct.* **2004**, *702*, 61−70. (b) Stamatatos, T. C.; Abboud, K. A.; Christou, G. *J. Chem. Soc., Dalton Trans.* **2009**, 41−50. (c) Graham, K.; Sharp, L. E.; Thomas, L. H.; Murrie, M. *Inorg. Chem. Commun.* **2012**, *25*, 89−91.

(14) (a) Ferguson, A.; Parkin, A.; Murrie, M. *J. Chem. Soc., Dalton Trans.* **2006**, 3627−3628. (b) Ferguson, A.; McGregor, J.; Parkin, A.; Murrie, M. *J. Chem. Soc., Dalton Trans.* **2008**, 731−733.

(15) (a) Evans, D. F. *J. Chem. Soc.* **1959**, 2003−2005. (b) Schubert, E. M. *J. Chem. Educ.* **1992**, *69*, 62. (c) Girolami, G. S.; Rauchfuss, T. B.; Angelici, R. J. *Synthesis and Technique in Inorganic Chemistry: A Laboratory Manual,* 3rd ed.; University Science Books: Sausalito, CA, 1999.

(16) Grant, D. H. *J. Chem. Educ.* **1995**, *72*, 39−40.

(17) Bain, G. A.; Berry, J. F. *J. Chem. Educ.* **2008**, *85*, 532−536.

(18) Bruker. *APEX2*; Bruker AXS Inc: Madison, WI, 2007.

(19) Sheldrick, G. M. *SADABS*; Bruker AXS Inc: Madison, WI, 1996.

(20) Sheldrick, G. M. *TWINABS*; University of Göttingen: Germany, 1996.

(21) Sheldrick, G. M. *Acta Crystallogr., Sect. A: Found. Adv.* **2015**, *71*, 3−8.

(22) Sheldrick, G. M. *Acta Crystallogr., Sect. A: Found. Crystallogr.* **2008**, *64*, 112−122.

(23) Farrugia, L. J. *J. Appl. Crystallogr.* **2012**, *45*, 849−854.

(24) Dolomanov, O. V.; Bourhis, L. J.; Gildea, R. J.; Howard, J. A. K.; Puschmann, H. *J. Appl. Crystallogr.* **2009**, *42*, 339−341.

(25) Brandenburg, K. *DIAMOND*; Crystal Impact GbR: Bonn, Germany, 1999.

(26) (a) Canty, A. J.; Minchin, N. J.; Skelton, B. W.; White, A. H. *J. Chem. Soc., Dalton Trans.* **1986**, 2205−2210. (b) Ünal, E. A.; Wiedemann, D.; Seiffert, J.; Boyd, J. P.; Grohmann, A. *Tetrahedron Lett.* **2012**, *53*, 54−55.

(27) Londregan, A. T.; Jennings, S.; Wei, L. *Org. Lett.* **2011**, *13*, 1840−1843.

(28) Boivin, J.; Carpentier, F.; Jrad, R. *Synthesis* **2006**, *2006*, 1664−1672.

(29) Yip, S. F.; Cheung, H. Y.; Zhou, Z.; Kwong, F. Y. *Org. Lett.* **2007**, *9*, 3469−3472.

(30) If needed, the A$_4$[PY(CO$_2$)$_4$] salts can be stored overnight in a −20 °C freezer before metalation.

(31) Detailed crystallographic information for all [PY(CO$_2$)$_4$]$^{4−}$ complexes can be found in Table S6.

(32) Mn: (a) Baca, S. G.; Malaestean, I. L.; Keene, T. D.; Adams, H.; Ward, M. D.; Hauser, J.; Neels, A.; Decurtins, S. *Inorg. Chem.* **2008**, *47*, 11108−11119. (b) Déniz, M.; Hernández-Rodríguez, I.; Pasán, J.; Fabelo, O.; Cañadillas-Delgado, L.; Yuste, C.; Julve, M.; Lloret, F.; Ruiz-Pérez, C. *Cryst. Growth Des.* **2012**, *12*, 4505−4518. (c) Chen, S.; Cheng, M.; Ren, Y.; Tang, L.; Liu, X.; Zai, C.; Liu, Q. *Z. Anorg. Allg. Chem.* **2015**, *641*, 610−616. Fe: (d) Laine, P.; Gourdon, A.; Launay, J.-P. *Inorg. Chem.* **1995**, *34*, 5129−5137. (e) Yoon, S.; Lippard, S. J. *J. Am. Chem. Soc.* **2005**, *127*, 8386−8397. Co: (f) Stamatatos, T. C.; Dionyssopoulou, S.; Efthymiou, G.; Kyritsis, P.; Raptopoulou, C. P.; Terzis, A.; Vicente, R.; Escuer, A.; Perlepes, S. P. *Inorg. Chem.* **2005**, *44*, 3374−3376. (g) Grirrane, A.; Pastor, A.; Álvarez, E.; Mealli, C.; Ienco, A.; Rosa, P.; Galindo, A. *Eur. J. Inorg. Chem.* **2007**, *2007*, 3543−3552. (h) Lian, Z.; Zhao, N.; Liu, P. *Z. Kristallogr. - New Cryst. Struct.* **2010**, *225*, 371−373. Ni: (i) Alexiou, M.; Dendrinou-Samara, C.; Raptopoulou, C. P.; Terzis, A.; Tangoulis, V.; Kessissoglou, D. P. *Eur. J. Inorg. Chem.* **2004**, *2004*, 3822−3827. (j) Yang, A.-H.; Zhang, H.; Gao, H.-L.; Zhang, W.-Q.; He, L.; Cui, J.-Z. *Cryst. Growth Des.* **2008**, *8*, 3354−3359. (k) Zhang, Y.-J.; Wang, J.-J.; Chen, J. Z. *Z. Anorg. Allg.*

Chem. **2012**, *638*, 1849−1854. Zn: (l) Chen, Z.; Gao, D.-L.; Diao, C.-H.; Liu, Y.; Ren, J.; Chen, J.; Zhao, B.; Shi, W.; Cheng, P. *Cryst. Growth Des.* **2012**, *12*, 1201−1211. (m) Faure, R.; Loiseleur, H. *Acta Crystallogr., Sect. B: Struct. Crystallogr. Cryst. Chem.* **1972**, *28*, 811−815. (n) Zhang, L.; Lin, Q.-P.; Li, Z.-J.; Zhang, J.; Qin, Y.-Y.; Cheng, J.-K.; Yao, Y.-G. *CrystEngComm* **2009**, *11*, 1201−1203.

(33) (a) Figgis, B. N.; Lewis, J. The Magnetic Properties of Transition Metal Complexes. In *Progress in Inorganic Chemistry*; Cotton, F. A., Ed.; Wiley: Chichester, U.K., 1964; pp 37−239. (b) *Encyclopedia of Inorganic Chemistry*, 2nd ed.; King, R. B., Ed.; Wiley: Chichester, U.K., 2005.

(34) Subtle changes in the color of solid samples of the complexes were also observed—from purple (Na$^+$) to purple-blue (Li$^+$ and K$^+$) to blue (Cs$^+$)—and were confirmed by minor changes in the diffuse reflectance spectra of these compounds in the solid state. In particular, the two maxima at 573 and 915 nm in the Na$^+$ spectrum were noticeably blueshifted in comparison to the maxima of the other three (Figure S14). Yet, the complexes exhibit identical solution UV−vis−NIR spectra (Figure S15). Thus, the minor differences in coloration of the solid samples likely arises from packing effects.

(35) Channel dimensions were calculated using Diamond.

(36) Further discussion of [(PY(CO$_2$)$_4$)Co(OH)]$^{2−}$ can be found in the Supporting Information.